Molecular Orientation and Anisotropic Charge Transport in the Large Area Thin Films of Regioregular Poly (3-alkylthiopnes) Fabricated by Ribbon-Shaped FTM

doi: https://doi.org/10.1016/j.orgel.2020.105687

Molecular Orientation and Anisotropic Charge Transport in the Large Area Thin Films of Regioregular Poly(3-alkylthiopnes) Fabricated by Ribbon-Shaped FTM

Atul S. M. Tripathi[1], Rakesh Kumar Gupta[1], Shubham Sharma[1], Shuichi Nagamatsu[2], and Shyam S. Pandey[1*]

[1]Graduate School of Life Science and Systems Engineering, Kyushu Institute of Technology, 2-4 Hibikino, Wakamatsu, Kitakyushu 808-0196, Japan

[2]Department of Computer Science and Electronics, Kyushu Institute of Technology, 680-4 Kawazu, Iizuka, 820-8502, Japan

E-mail: shyam@life.kyutech.ac.jp

Abstract

Introduction of alkyl chains is a plausible approach to impart the facile solution processability in regioregular poly (poly-3-alkylthioness) (RR-P3ATS) but drastic fall in the conductivity as a function of increasing alkyl chain length restricted the versatile use of its hexyl substituted derivative (P3HT). In this work, fabrication of large area oriented thin films of RR-P3ATs with varying alkyl chain lengths was successfully demonstrated using ribbon shaped floating film transfer method (FTM). Observed decrease in the molecular orientation with increasing alkyl chain length was explained by enhanced alkyl chain inter-digitation as evidenced by trends of d-spacing estimated from the out-of-plane XRD results. In-plane GIXD revealed edge-on orientation in the thin films of all of the P3ATs prepared by ribbon-shaped FTM, which is highly desired for planer charge carrier transport. Parallel oriented thin film of longest alkyl chain

(octadecyl) substituted P3AT poly (3-octadecylthiophene) exhibited a field effect transistor (FET) mobility of 1.9 x 10^{-2} cm^2/Vs, which is about 4-5 orders of magnitude higher as compared its previously reported values estimated by time-of-flight and FET methods. Thus, fabrication of thin films by FTM leads to versatile choice of RR-P3ATs for solution processing for FETs using common organic solvents without having any detrimental impact of alkyl chain length on the charge carrier mobility.

Keywords: Poly(3-alkylthiophene), Floating film transfer, Orientation, Polarized absorption, Anisotropic charge transport, Field effect transistors

Introduction

Last two-decades have witnessed a tremendous growth in the ever growing field of conjugated polymers (CPs) owing to their utilization as active organic semiconductor elements in diverse area of applications such as organic field effect transistors (OFET) [1-3] photovoltaic cells [4-5] and organic light emitting diodes [6-7] etc. Synthetic versatility, light weight, incorporation of desired functionality (n-type or p-type), energetic control in combination with solution processability of CPs have led to the emergence of new area of the organic electronics. Amongst the various CPs developed so far since its inception in 1977 as polyacetylene, thiophene class of polymers/copolymers has been most extensively studied in the area of organic electronics. Especially, after introduction of the regiocontrolled (head-to-tail coupling) in the poly(3-alkylthiophenes) (P3ATs) [8-9], there was a surge in the utilization of this class of materials as active semiconductor elements in various organic electronic devices. This was not only due to their excellent solubility in common organic solvents but also superior charge transport as compared to their non-regiocontrolled P3ATs counterparts synthesized by traditional oxidative polymerization using $FeCl_3$. Introduction of alkyl group at 3-position in the Regioregular (RR) P3ATs although imparted the enhanced solution processability but led to the hampered charge transport as a function of increasing alkyl chain length [10-11]. This is the reason why, RR-poly(3-hexylthiophene) (P3HT) is still one of preferred choices amongst the RR-P3ATs owing to an amicable balance between the facile solution processability as well as the charge transport.

OFETs utilizing thin films of CPs can be considered as backbone of the organic electronic devices and controlling their cost and performance is inevitable for the practical realization of the organic electronics. In this context, performance can be controlled by the nature

of CPs and quality of the thin films, while cost largely depends on the methods adopted for the thin film fabrication. Owing to the planer device architecture of OFETs a very thin homogeneous film is undoubtedly desired but at the same time aligning the CPs in the channel direction (from source-drain) boosts the device performance. Quasi 1-dimensionality of CPs along with extended π-conjugation offer them an inherent capability of molecular self-assembly and uniaxial alignment of the macromolecular domains. Usually, thin films of CPs fabricated by solution process exhibit semi crystalline structure having crystalline domains distributed in the amorphous disordered matrix [12-13]. This disorder is responsible for the hampered device performance by posing the adverse effect for efficient charge carrier hopping between transport locations [13-14]. Therefore, thin film fabrication methods having capability of molecular orientation are highly advantageous for the organic electronic devices especially the OFETs [15]. In spite of the fact that spin-coating being most commonly implemented method for device applications, large material wastage and isotropic film morphology led to the proposal of different methods involving promotion of molecular self-assembly and imparting the molecular orientation. To address these issues of thin film fabrication, a number of methods such as dip coating [16], solution flow [17], bar coating [18], strain alignment [19], mechanical rubbing [20] and friction transfer [21] etc. have been proposed. Although, these methods are successful towards the solution of problem faced by spin-coating, but intriguing issues like mechanical and compositional damage along with damage of under layer by upper layer in the case of multilayer film fabrication needs further attention.

To resolve such issues for the thin film fabrication of solution processable CPs, our group have developed a technique for the facile fabrication of thin films on any desired substrate by

casting a polymer solution on an orthogonal liquid substrate named as dynamic floating film transfer method (FTM) [22-23]. FTM not only provide multilayer thin films with minimal material wastage but also imparts the orientation in the fabricated thin films [24]. Conventional FTM leads to circular thin films due to spreading of the films in all directions and films on outer ends are relatively thin and more oriented. To resolve this issue, we further improvised this method using an assisting slider to provide directionality during spreading of the polymer solution leading to large area ribbon shaped thin films named as ribbon shaped FTM [25-26]. In this work, we would like to report about the anisotropic optical and electrical characterizations of large area thin films of the RR-P3ATs (A= butyl, hexyl, octyl, decyl, dodecyl and octadecyl) fabricated by ribbon shaped FTM. Fabricated thin films have been variously characterized using polarized absorption spectroscopy, out-of-plane and in-plane grazing incident X-ray diffraction followed by anisotropic charge transport after the fabrication of OFETs using these oriented thin films. Influence of the alkyl chain length on optical anisotropy and molecular ordering in these films has been investigated in detail. It has been demonstrated that charge carrier mobility does not sharply decrease as function of alkyl chain length contrary to the previous reports [10-11] owing to the adoption of edge on orientation promoting in-plane charge transport in the OFETs.

2. Experimental:

2.1 Materials and methods

The RR-P3ATs having head to tell (HT) coupling >98 in case of hexyl (C6; P3HT), decyl (C10; P3DT), dodecyl (C12; P3DDT) and octadecyl (C18; P3ODT) and 80-90% in case of butyl substituted (C4; P3BT) polythiophenes, dehydrated chloroform and toluene were purchased from

Sigma Aldrich. Respective CP solutions with concentration of 2 % and 0.5 % (w/w) were prepared by dissolving in dehydrated chloroform for thin film fabrication by FTM and spin coating, respectively. Large area oriented thin films of P3ATs were prepared by ribbon shaped FTM as per our earlier publications [25-26, 27-28]. For comparison, non-oriented spin coated thin films were also prepared by spinning the chloroform solution of respective CPs at 3000 rpm for 120 sec. The oriented films prepared by ribbon shaped FTM were transferred on the substrates like glass and SiO_2 coated silicon wafer for optical and electrical characterizations, respectively. For the XRD measurements, thin film samples were prepared on to hexamethyldisilazane (HMDS) treated silicon substrates by multi-layer thin film casting using FTM in order to get significant XRD signals [29]. Out-of-plane XRD measurements were carried out using a Rigaku X-ray diffractometer with Cu-Kα radiation operating at 40 kV and 20 mA. For in-plane GIXD, a Rigaku smart lab was used. The in-plane incident angle was kept above the critical angle of the substrate, and the diffraction measurement was carried out both parallel and perpendicular to the polymer orientation directions, as reported earlier [30]. Polarized electronic absorption spectra were measured by UV-visible spectrophotometer (JASCO V-570) equipped with a Glan-Thompson prism. In order to measure the optical anisotropy, rotating polarizer was used before the detector that was rotated to change the polarization directions. Optical anisotropy in terms of dichroic ratio (DR) was estimated from the polarized absorption spectra and calculated by the relation $DR = A_{\parallel}/A_{\perp}$ where, $A_{\parallel}$ and $A_{\perp}$ indicate the maximum absorbance, when polarization direction was $\parallel$ to $\perp$ to the film orientation direction, respectively.

2.2 OFET fabrication and its characterization

For electrical characterization, OFETs were fabricated by using highly doped p- type Si substrate with 300 nm thermally grown SiO_2 insulating layer having capacitance (C_i= 10 nf/cm^2) and thin films of P3ATs as active organic semiconductor with molecular structure as shown in the Fig. 1(a). SiO_2 surface was treated by octadecyltrichlorosilane (OTS) for the formation of hydrophobic self-assemble monolayer, which assists the better adhesion of the P3ATs during thin film fabrication on the SiO_2 insulator. Although both HMDS and OTS surface treatments of SiO2 has been frequently used for providing surface hydrophobicity allowing self-assembly of hydrophobic alkyl chains of CPs, longer alkyl chain of OTS are expected to provide relatively better self-assembly of P3ATs especially the polymers having longer alkyl chain lengths. Lim et al have also reported that as compared HMDS, OTS surface treatment of SiO_2 gate insulator led to nearly to fold enhancement in the charge carrier mobility due to promoted self-assembly of the macromolecules [31] To accomplish this, Si substrates were dipped in 8 mM OTS solution in dehydrated toluene at 90^{o}C for 2 hours followed by washing with toluene and drying at 130^{o}C. Oriented floating films of P3ATs were transferred on OTS treated SiO_2/Si substrates by stamping. OFETs were fabricated in bottom gate top contact (BGTC) device architecture as shown in the Fig. 1(b). 50 nm to source and drain gold electrodes were deposited at the rate of 1.5 Å/s by a thermal evaporator with high vacuum of 10^{-6} torr using nickel shadow mask. In order to make parallel and perpendicular OFETs for the investigation of anisotropic charge transport, direction of the mask was accordingly selected (considering direction of orientation in the film) to deposit top source-drain electrodes. The channel length (L) and width (W) was fixed for all of devices to be 20 µm and 2 mm, respectively. Electrical characterizations were done by computer controlled 2 channel electrometer (Kiethley 2612) at vacuum of 10^{-3} Pa.

3. Result & Discussion

3.1 Large area thin film preparation by ribbon shaped FTM

It has been already reported by our group that conventional FTM leads to multidirectional film spreading, while higher orientation and uniformity was observed towards the outer ends. This led to proposal of the improvised ribbon shaped FTM, resulting in to large area rectangular ribbon shaped floating films [25]. Extent of the orientation, thickness and size of film were controlled by casting parameters such as concentration of polymer solution, casting temperature and viscosity of liquid substrate etc. [25,32]. In this study, a series of alkyl chain substituted RR-P3ATs were used for the fabrication of large area oriented thin films and their utilization for opto-electrical characterizations. Main reason to utilize different alkyl chains for investigation was to harness the facile solubility of these CPs in common organic solvents as function of increasing length of alkyl side chains [10]. For making thin films under ribbon shaped FTM, a 20-25 µl of polymer solution in chloroform was dropped in the center of slider, which was dipped in a rectangular tray (15 cm x 25 cm) with partly filled hydrophilic liquid substrate consisting of binary liquid mixture of ethylene glycol and Glycerol in the ratio of 3:1 (v/v). The dipped slider was placed at one end of the tray in such a manner that half of the slider remains in the liquid substrate. When polymer solution starts spreading, bottom walls of the slider provide the directionality to the spreading film propagating in one direction and make a solid film on liquid substrate like a large ribbon as shown in the Fig. 2.

Key feature of this method lies in the fact that film was prepared by natural self-assembly process without any external force or controlling setup like Langmuir-Blodgett (LB) films. In this method, fabricated thin films get aligned by dynamic solvent evaporation followed by

solidification during spreading and compressive force by viscous liquid substrate in opposite direction. The film orientation was observed to be perpendicular to the direction of the solution spreading as verified by the polarizer film. It can be clearly seen that all of P3ATs under investigation form large area thin films (> 2 cm x 20 cm), which are ready for transfer on any desired substrate for further characterization and applications. Large area further facilitates to prepare thicker films also by multiple stamping, which is desired for characterizations like XRD or polarized FTIR to acquire measurable signal intensity [33].

3.2 Optical Characterization

Electronic absorption spectra of RR-P3ATs prepared by spin-coated thin films was first recorded and analyzed in order to investigate the implications of alkyl chain length and molecular ordering on the optical properties. Solid-state electronic absorption spectra of spin-coated thin films RR-P3ATs is shown in the Fig. 3(a). It is well-known that thin film absorption spectra of RR-P3ATs typically exhibit absorption maximum (λ_{max}) after 500 nm associated with π-π^* electronic transition followed by vibronic shoulders around 550 nm and 600 nm associated molecular packing and enhanced intermolecular interactions due to lamella formation [34]. A perusal of Fig. 3(a) indicates that there is gradual red-shift in the λ_{max} of RR-P3ATs as function increasing alkyl chain length form butyl (C4) to dodecyl (C12) appearing at 506 nm, 530 nm, 536 nm, 538 nm, respectively, along with appearance and red-shift of vibronic shoulders. This red-shift indicates the extension of molecular ordering as a function of increasing alkyl chain length, which might be associated of increased inter-molecular interactions in the condensed state. Interestingly, as cast spin coated thin film of octadecyl (C18) substituted P3ODT exhibited a featureless

absorption spectrum having λ_{max} at 510 nm and there was a pronounced red-shift with very clear vibronic shoulders after annealing the film at 100^{o}C for 30 min. This could be attributed to the fact that too long alkyl substitution initially hinder the molecular packing in solid-state but annealing promotes the molecular ordering by enhanced alkyl chain inter-digitation leading to this pronounced red-shift associated with enhanced intermolecular interactions. Another possibility of such a drastic change in the case of P3ODT could be attributed to solid-liquid phase transition. Tada et al have also reported that this polymer starts melting around 100^{o}C [35]. Therefore, annealing at 100^{o}C leads to first melting of the alkyl chains and upon cooling these alkyl chains undergo thermodynamically favorable inter-chain interactions leading to the chain inter-locking.

A representative polarized electronic absorption spectra of hexyl (C6) substituted P3HT prepared by ribbon-shaped FTM has been shown in the Fig. 3(b). A perusal of this figure clearly corroborates that there is marked difference in the spectral feature, when angle of incident beam on the film was changed from 0^{o} to 90^{o} indicating the presence of optical anisotropy due to molecular orientation having a dichroic ratio (DR) of 2.1. It is worth to mention that vibronic features are much clear in the oriented thin films prepared at room temperature without any annealing as compared to its spin-coated counterparts shown in the Fig. 3(a). This indicates that orientation promotes the molecular ordering, which was further validated considering the fact that in the parallel oriented thin film this vibronic shoulder becomes more pronounced as compared to main peak appearing around 520 nm associated with the π-π^* electronic transition. Takashima et al have also observed that vibronic shoulder around 550 nm get more pronounced as compared to the main peak appearing around 520 nm in the drop costed thin films of P3HT as

compared to its spin-coated thin film counterparts, which was explained by enhanced molecular ordering [36]. A similar spectral behavior in the oriented thin films of RR-P3HT prepared by conventional FTM with DR of 1.8 has also been observed by our group previously [37].

Oriented thin films of RR-P3ATs prepared by ribbon-shaped FTM were also characterized by polarized electronic absorption spectroscopy in order to investigate the implication of alkyl chain length on anisotropic optical properties and extent of molecular orientation. Normalized electronic absorption spectra of RR-P3ATs in their parallel orientation is shown in the Fig, 4(a). A differential spectral behavior for parallel FTM with respect to their corresponding spin coated counterparts can be clearly seen. In this series of P3ATs, λ_{max} for the parallel FTM films was found at 516 nm, 542 nm, 554 nm, 552 nm and 562 nm for the C4, C6, C10, C12 and C18 alkyl substituted P3AT, respectively. This red-shift in the $\lambda_{max,}$ relatively more pronounced vibronic features for the thin films fabricated at room temperature and red-shift in the optical absorption edges (650 nm-680 nm) as compared to spin-coated thin film counterparts (640 nm-660 nm) clearly corroborates the molecular self-assembly and orientation induced extended π-conjugation in these FTM processed RR-P3AT thin films.

Polarized absorption spectrum of the corresponding RR-P3ATs processed by ribbon-shaped FTM was subjected to quantitative estimation of extent of molecular orientation by calculating the optical anisotropy in the films. This optical anisotropy was quantified in terms of DR, which was calculated by the ratio of maximum absorbance parallel at $\lambda_{max}\parallel$ to absorbance in perpendicular at $\lambda_{max}\parallel$ by the relation ($DR= A_{\parallel}/A_{\perp}$). Figure 4(b) depicts the influence of the

substituted alkyl chain length of P3ATs on the extent of the molecular orientation observed in these oriented thin films. A perusal of this figure reveals that DR in the thin films first increases form C4 (1.2) to C6 (2.2) followed by concomitant decrease upon further increase in the alkyl chain length from C10 to C18. It was thought that increase in the flexible and mobile alkyl chain length may lead to enhanced DR for thin films fabricated by the FTM but it was rather opposite. To explain this unusual behavior of alkyl chain length dependent molecular orientation, microstructural characterization using out-of-plane XRD and in-plane GIXD measurements were also conducted, which will be discussed in detail in the next section.

3.3 Out-of-plane XRD and in-plane GIXD measurements

Oriented thin films of the P3ATs prepared by ribbon-shaped FTM transferred on silicon wafer were further subjected to both of the in-plane and out-of-plane modes by XRD in order to investigate the polymeric stacking and backbone conformations. As schematically shown in the Fig. 5(a), thin film was examined in the three different directions, which was defined as the difference between the incident and scattered X-ray wave vectors [38]. The scattering vector Q was defined as $Q = 4\pi(\sin\theta)/\lambda$, where, θ and λ are the Bragg angle and wavelength of the incident X-ray, respectively. The out-of-plane X-ray scattering vector q_z and the in-plane X-ray scattering vector q_{xy} were positioned perpendicular and parallel to the film surface, respectively. Angle χ between the in-plane scattering vector and the orientation direction of the FTM processed film was fixed during the in-plane ϕ-$2\theta_\chi$ scans. χ is related to the scattering vectors q_x and q_y for fixed χ angles of 0^o and 90^o, respectively. For both of the out-of-plane 2θ and the in-plane ϕ-$2\theta_\chi$ scans, scanning speed and angular intervals were fixed to be 2^o/min and 0.02^o,

respectively. A perusal of the out-of-plane XRD profile shown in the Fig. 5(b) (qz-red line) reveals the presence of all of the clear diffraction peaks for the lamellar stacking of the hexyl side chains of RR-P3HT appearing at 5.35^{o}, 10.70^{o} and 16.05^{o} associated with the 100, 200 and 300 diffractions.

The d-spacing calculated from shift between the 100 and 200 peaks using Scherer equation was found to be 16.51 Å, which was slightly lower than reported for the spin-coated films of RR-P3HT (16.95 A) reported by our group. At the same time, peaks are more pronounced up to higher order as compared to that reported for spin-coated films indicating enhanced crystallinity in these FTM processed films [39]. Interestingly, the in-plane GIXD profile shown in the Fig. 5(b) (blue and black lines) does not exhibit the peaks associated with alkyl chains rather exhibit one peak appearing at 2θ of 23.19^{o} corresponding to the π-π stacking. Therefore, presence peak associated mainly with π-π stacking and absence of any diffraction peaks associated with (h00) of alkyl side chains clearly corroborates the presence of edge-on conformation of the macromolecules in the thin films of the RR-P3HT prepared by ribbon shaped FTM.

Figure 6(a) depicts the out-of-plane XRD of RR-P3ATs thin films with varying alkyl chain length prepared by ribbon-shaped FTM. A perusal of the XRD profile clearly corroborates the appearance of clear peaks up to higher orders indicating the lamella formation by stacking of the alkyl chains. It can also be seen that there is a gradual decrease in the all of peaks associated with of h00 with the increasing length of the alkyl substituents. Interestingly, these higher order

peaks such as 200 and 300 becomes even more pronounced in the case of P3ATs with longer alkyl chain lengths. Exact origin for the pronounced higher order peaks especially 300 for P3ATs with longer alkyl chain substituents is although not completely clear but it could be associated with enhanced crystallinity of the macromolecules promoted by alkyl chain stacking via inter-digitation. This explanation seems to be plausible considering the result reported by Nieuwendaal et al about processing induced differential crystallization of RR-P3HT as probed by XRD and DSC differential scanning calorimetric investigation [40]. In this interesting report authors have demonstrated that fast dried thin films RR-P3HT exhibited only 100 peak while slow dried thin film exhibited diffraction peaks up to higher orders, where 300 peak was relatively more pronounced as compared to its 200 peak counterparts. Therefore, slow drying leads to enhanced crystal packing of macromolecules, where alkyl chains undergo self-organization in the thermodynamically more favorable states. Takashima et al [36] have also reported out-of-plane XRD profile of the spin-coated thin films of RR-P3ATs with clear 100 peaks mainly towards lower 2θ but presence of clear peaks up to higher orders in the present work indicates that FTM processed films have relatively higher crystallinity. This is attributed to the increased interaction between the alkyl chains of the polymeric molecules imparting the enhanced possibility alkyl chain inter-digitation. In-plane GIXD as shown in the Fig. 6(b) clearly reveals complete absence of diffraction peaks associated with alkyl-side chain stacking confirming the presence of edge-on conformation in the case of all of the P3ATs prepared by FTM and used for the present investigation. In order to confirm the enhanced alkyl chain interaction and alkyl chain inter-digitation for the RR-P3ATs with the increasing alkyl chain lengths, d-spacing was calculated from the out-of-plane XRD profile using Scherer equation.

Dependence of the calculated d-spacing as function of alkyl chain length in the RR-P3AT thin films has been shown in the Fig. 7(a).

It has been reported that in the case of the molecular packing of long alkyl chain fatty acids in a normal bilayer format, there is an increase in the d-spacing of 2.54 Å/CH_2 units, since increasing the length of each acyl chain by one CH_2 unit results in to an increase in the d-spacing by 1.27 Å [41]. Therefore, theoretical values of d-spacing for RR-P3ATs in this work was calculated taking normal bilayer packing of alkyl chains of the P3ATs along with addition of 3.80 Å for the thienyl ring packing as reported by Takashima et al. [36] Theoretical d-spacing data was plotted for alkyl substituted P3ATs considering lipid bilayer like packing of alkyl chains in the P3ATs (blue line) as shown in the Fig. 7(a) exhibits the linear dependence as function of increasing CH_2 unit having slope of 2.54 Å/CH_2. Contrary to this, experimental values of the d-spacing estimated from the XRD profile exhibits sublinear dependence of the d-spacing having the slope of 1.65 Å as a function of the increasing number of carbon atoms in the alkyl chains of the RR-P3ATs (red line). Therefore, deviation from linearity in the d-spacing for RR-P3ATs thin films fabricated by FTM suggests that arrangement of the alkyl chains is not like lipid bilayer rather inter-digitated, whose extent increases as a function of increasing alkyl chain length as shown schematically in the Fig. 7(b). In the previous section, it has been discussed that although ribbon-shaped FTM provided large area uniform and oriented thin films for all of the RR-P3ATs but extent of molecular orientation decreases as a function of increasing alkyl chain length as shown in the Fig. 4(b). This can be well explained by increase in the extent of the inter-digitation of the alkyl chains as a function of increasing alkyl chain length, which provide stiffness to the macromolecules. This increased inter-digitation poses hindrance for the

orientation by the opposing viscous dragging force during the film formation during the FTM. This explanation seems to be plausible considering the fact that stiff molecules like RR-P3HT and PBTTT are less prone to the orientation under FTM as compared to the flexible non-regiocontrolled P3HT as reported by our group previously [35].

3.4 Anisotropic charge transport in RR-P3ATs

After the successful fabrication of large area and oriented thin films of RR-P3ATs by ribbon-shaped FTM, they were subjected to investigation of anisotropic charge transport after fabrication of OFETs in the BGTC device architecture as shown in the Fig. 1(b). Although OFETs in the bottom gate bottom contact (BGBC) device configuration have also been reported in literature but in the present work, BGTC device architecture was adopted owing to wide spread applicability of SiO_2 as gate insulator, easy availability form various commercial sources and least damage to dielectric layer using solution processable organic semiconductors. At the same time, Bhargava et al have also advocated the superiority of BGTC device architecture over its BGBC counterparts due to small contact resistance based on their two dimensional optoelectronic simulations [42]. Figure 8 depicts the typical output and transfer characteristics of oriented thin films of RR-P3HT in the case of parallel and perpendicular orientation with respect to channel direction. A perusal of this figure corroborates a clear p-type transistor behavior, when gate to source voltage (V_{GS}) varied from 0 to -80 V. Apart from p-type behavior (driving the OFET by negative gate biasing), it can be seen that there was enhanced drain current (I_D) for parallel OFETs as compared to that of its perpendicular device counterparts at each respective gate to source voltage (V_{GS}) reflecting anisotropic charge transport.

Field effect mobility (μ) was calculated from the transfer curve, when drain current start to saturate at condition $V_{DS} \geq V_{GS}-V_{th}$ and constant current flow in channel using the following equation 1.

$$\mathbf{I_D = \frac{1}{2}\ \mu_n\ C_{ox}\ \frac{W}{L}\ [V_{GS} - V_{th}\ ]^2} \quad \text{.....} \quad \mathbf{(1)}$$

Where, I_D, W, L, μ, C_{ox}, V_{GS} and V_{th} are, saturated output current, channel width, channel length, charge carrier mobility, capacitance of gate insulator, applied gate bias voltage and threshold voltage, respectively. Transfer curve (I_{DS} $-V_{GS}$) and ($I_{DS}^{1/2}$-V_{GS}) of the OFETs operated at VGS=−80 V as shown in the Fig. 8(b) was utilized to extract the electrical parameters of the OFETs. Estimation of FET mobility of RR-P3HT from the Fig. 8(b) gives the value of 3.0 x 10^{-2} cm^2/V.s for parallel oriented film (**$\mu_{\parallel}$**), which was 1.8 times higher as compared that of its perpendicular oriented (**$\mu_{\perp}$**) OFET counterparts (1.7 x 10^{-2} cm^2/V.s) with on/off ratio ($\frac{I_{on}}{I_{off}}$), of 10^4 justifying the anisotropic charge transport. Small electrical anisotropy (**$\mu_{\parallel}/\mu_{\perp}$**) of 1.8 observed for RR-P3HT is attributed to the small optical anisotropy (DR=2.2) as shown in the Fig. 4(b). Parallel and perpendicular OFETs for all of RR-P3ATs were also fabricated in BGTC device architecture in order to investigate the implication of alkyl chain length on the charge carrier mobility and anisotropic charge transport. Uniform and oriented thin films of RR-P3ATs in each case were fabricated by ribbon-shaped FTM. Electrical parameters like μ, ($\frac{I_{on}}{I_{off}}$), electronic anisotropy ($\mu_{\parallel}/\mu_{\perp}$) etc. estimated from the transfer curves for all of the CPs along with corresponding optical anisotropy (DR) have been summarized in the table 1.

A perusal of the table 1 clearly corroborates that in all of RR-P3ATs prepared by ribbon-shaped FTM, carrier mobility in the case of parallel OFETs is higher as compared to that of their corresponding perpendicular OFET counterparts indicating anisotropic charge transport with mobility anisotropy varying between 1.2 to 1.8 and follows the nearly same trend of optical anisotropies. Small variation in extent of optical and electrical anisotropies as function of alkyl chain length in the RR-P3ATs make us difficult for concrete discussion about the general trend that higher optical DR leads to higher mobility anisotropy. At the same time, RR-P3HT having smallest alkyl chain substitution reveals a clear opposite trend, where higher electrical anisotropy was observed in spite of its low DR. Presumably, lack of long alkyl chains in the P3BT promotes strong π-π interactions leading to more rod like confirmation as compared to random coil and this rod-like molecular self-assembly could be responsible for relatively higher electrical anisotropy. This could be further supported by fact that from o-dichlorobenzene solution, P3BT easily form nanowires while P3HT needs some poor solvent additive like cyclohexanone [43-44].

The relatively small values of the optical anisotropy observed in all of the cases is associated with the higher crystallinity of the films owing to regioregularity and alkyl chain interdigitation as reported by us previously [37]. It is very interesting to mention here that alkyl chain substitution in RR-P3ATs although exhibit slight decrease in the field effect mobility following the decreasing trend of DR but surprisingly very small as compared to that of previous reports on alkyl chain length dependent charge carrier motilities in the RR-P3ATs [10-11,36]. It is worth to mention here that Babel et al reported a three orders of magnitude decrease in the FET mobility of RR-P3ATs upon increasing the alkyl chain length from hexyl to dodecyl [11]. Similarly, Takashima et al and Kaneto et al have also reported a drastic decrease (about 4 orders of magnitude) in the carrier mobility in RR-P3ATs upon increasing the alkyl chain length as

studied by time-of-flight (TOF) (sandwich configuration) and FET (planer configuration) fabrication, respectively [10,45]. It needs special mention here that this hampering in the mobility was even more drastic (about 2 orders of magnitude) upon increasing the length of alkyl chains from C12 (dodecyl) to C18 (octadecyl).

It is well known that introduction of alkyl chains in the P3ATs was made aiming towards increasing their solubility in common organic solution for the easy fabrication of the thin films using solution based approaches. At the same time, a drastic decrease in the carrier mobility after hexyl substitution as discussed above led to the most versatile use of the P3HTs for the device applications restricting the use of other P3ATs in spite of their enhanced solubility. Contrary to this, OFETs based on ribbon-shaped FTM processed thin films of P3ATs exhibited very small influence of alkyl chain substitution on the observed carrier mobility as show in the table 1. This clearly indicates that using FTM, it is possible to harness the alkyl chain substitution dependent beauty of solubility of P3ATs in common organic solvents without having any serious detrimental effect on charge transport in the planer organic electronic devices like OFETs. Therefore, it is interesting to throw light about such a contrasting difference on the alkyl chain length dependent carrier motilities reported previously by many groups including us and the that being reported in this present work. This can be explained considering the nature of charge transport in device under consideration and orientations/conformations of macromolecules on the substrate as shown schematically in the Fig. 9.

It has been reported that P3ATs adopt different types of conformation as face-on, edge-on or end-on depending on the structure of macromolecules, method of thin film fabrication and nature/concentration of solvents used for preparation of polymer solution [21, 46-47]. In the face-on conformation of P3ATs, both of the polymeric backbone and alkyl side chains are present in the same plane of the substrate, therefore in-plane charge transport is hindered exhibiting strong alkyl chain length dependent of mobility and such a conformation is suitable for vertical devices like diodes and solar cells. Contrary to this, in the face-on conformation, alkyl chain staking is orthogonal to the substrate plane and in-plane charge transport is highly favorable having least influence of alkyl chain length in the polymer backbone plane, which is highly beneficial for devices like OFETs [48]. Utilizing TOF method for investigating the charge transport in RR-P3ATs, it was previously reported that film prepared by spin coating method exhibited not only the face-on orientation but also strong alkyl chain length dependent charge carrier mobility [10-11, 36]. On the other hand, we have previously demonstrated that edge-on was the preferred conformation in the thin films CPs like of P3ATs and others from thiophene family prepared by FTM film based on our out-of-plane XRD and in-plane GIXD investigations [26, 33, 46]. It is clear from the Fig. 6 that all of the RR-P3ATs under investigation, exhibited edge-on orientation where, the macromolecular π-stacking is parallel to substrate in the direction of source and drain electrodes leaving alkyl side chains orthogonal to the substrate. This allows facile in-plane charge carrier transport via inter molecular hopping having least hindrance in the charge transport by the length of alkyl side chains as shown schematically in the Fig. 9. A very strong alkyl chain length dependent charge carrier mobilities as discussed earlier is attributed to the attainment of the face-on orientation by the films prepared by spin-coating, where inter-chain hopping after the intra-chain transport has to be dictated by the alkyl chain length and there is

drastic hampering in the charge carrier transport as function of increasing alkyl chain length. This is further validated by report of Liu et al, who emphasized that in the alkyl thiol passivated PbSe nanocrystals, charge carrier mobilities decreases exponentially with increasing alkyl chain length of passivating ligands and explained considering the hopping transport in granular conductors with alkyl side chain tunnel barriers [49]. Therefore, it could be concluded that FTM provides the edge-on oriented large area thin films and lack of alkyl chain length dependent carrier mobility in OFETs allows to harness the full potential of alkyl chain assisted solubility in the common organic solvents without having any detrimental effect of the alkyl substituents on the charge carrier transport,

4. Conclusion

In summary, large area (> 2 cm x 20 cm) oriented thin films of RR-P3ATs with varying alkyl chain length (butyl to octadecyl) were successfully prepared by ribbon shaped FTM. Alkyl chain length dependent orientation was investigated by polarized electronic absorption spectra, where extent of orientation was found to decrease as a function of increasing alkyl chain length. This was explained considering the enhanced alkyl chain inter-digitation for long alkyl chain substituted P3ATs as evidenced by sublinear alkyl chain length dependence of the d-spacing estimated from the out-of-plane XRD results. In-plane GIXD results clearly corroborated the presence of edge-on orientation in the thin films for all of the P3ATs prepared by ribbon-shaped FTM. Thanks to the edge-on orientation, where alkyl chains perpendicular to the π-π stacking of polythiophene main chain leads to least influence of alkyl chain length dependent hampering in the planer charge transport. This was further verified by the fact that in spite of such a large

variation in the alkyl chain length, variation in the FET mobility of RR-P3ATs was within an order of magnitude only. Therefore, fabrication of thin films by FTM leads to the versatile choice of RR-P3ATs for solution processing for FETs using common organic solvents without having serious implication of alkyl chain length.

References

[1] B.G. Kim, E.J. Jeong, J.W. Chung, S. Seo, B. Koo, J. Kim, A molecular design principle of lyotropic liquid-crystalline conjugated polymers with directed alignment capability for plastic electronics, Nat. Mater. 12 (2013) 659–664. doi:10.1038/nmat3595.

[2] M. Ikawa, T. Yamada, H. Matsui, H. Minemawari, J. Tsutsumi, Y. Horii, M. Chikamatsu, R. Azumi, R. Kumai, T. Hasegawa, Simple push coating of polymer thin-film transistors, Nat. Commun. 3 (2012) 1–8. doi:10.1038/ncomms2190.

[3] H. Sirringhaus, Device physics of solution-processed organic field-effect transistors, Adv. Mater. 17 (2005) 2411–2425. doi:10.1002/adma.200501152.

[4] M.C. Scharber, On the Efficiency Limit of Conjugated Polymer:Fullerene-Based Bulk Heterojunction Solar Cells, Adv. Mater. 28 (2016) 1994–2001. doi:10.1002/adma.201504914.

[5] G. Li, R. Zhu, Y. Yang, Polymer solar cells, Nat. Photonics. 6 (2012) 153–161. doi:10.1038/nphoton.2012.11.

[6] A. Sandstrom, H.F. Dam, F.C. Krebs, L. Edman, Ambient fabrication of flexible and large-area organic light-emitting devices using slot-die coating, Nat. Commun. 3 (2012) 1-5 doi:10.1038/ncomms2002.

[7] J. Liang, L. Li, X. Niu, Z. Yu, Q. Pei, Elastomeric polymer light-emitting devices and displays, Nat. Photonics. 7 (2013) 817–824. doi:10.1038/nphoton.2013.242.

[8] T.A. Chen, X. Wu, R.D. Rieke, Regiocontrolled Synthesis of Poly(3-alkylthiophenes) Mediated by Rieke Zinc: Their Characterization and Solid-State Properties, J. Am. Chem. Soc. 117 (1995) 233–244. doi:10.1021/ja00106a027.

[9] R.D. Mccullough and R.D. Lowe, Enhanced electrical conductivity in regioselectively synthesized poly(3-alkylthiophenes),. J. Chem. Soc. Chem. Commun. 1 (1992) 70–72.doi: 10.1039/C39920000070

[10] W. Takashima, S.S. Pandey, T. Endo, M. Rikukawa, K. Kaneto, Effects of regioregularity on carrier transport in poly(alkylthiophene) films with various alkyl chain lengths, Curr. Appl. Phys. 1 (2001) 90–97. doi:10.1016/S1567-1739(00)00018-3.

[11] A. Babel, S.A. Jenekhe, Alkyl chain length dependence of the field-effect carrier mobility in regioregular poly(3-alkylthiophene)s, Synth. Met. 148 (2005) 169–173. doi:10.1016/j.synthmet.2004.09.033.

[12] H. Tanaka, M. Hirate, S. Watanabe, S. Kuroda, Microscopic Signature of Metallic State in Semicrystalline Conjugated Polymers Doped with Fluoroalkylsilane Molecules,26 (2014) 2376–2383. doi:10.1002/adma.201304691.

[13] A. Salleo, R.J. Kline, D.M. DeLongchamp, M.L. Chabinyc, Microstructural characterization and charge transport in thin films of conjugated polymers, Adv. Mater. 22 (2010) 3812–3838. doi:10.1002/adma.200903712.

[14] R. Noriega, J. Rivnay, K. Vandewal, F.P. V Koch, N. Stingelin, P. Smith, M.F. Toney, A. Salleo, A general relationship between disorder, aggregation and charge transport in conjugated polymers, Nat. Mater. 12 (2013) 1038–1044. doi:10.1038/nmat3722.

[15] F.C. Krebs, M. Hösel, M. Corazza, B. Roth, M. V. Madsen, S.A. Gevorgyan, R.R. Søndergaard, D. Karg, M. Jørgensen, Freely available OPV—The fast way to progress, Energy Technol. 1 (2013) 378–381. doi:10.1002/ente.201300057.

[16] S. Wang, A. Kiersnowski, W. Pisula, K. Müllen, Microstructure evolution and device performance in solution-processed polymeric field-effect transistors: The key role of the first monolayer, J. Am. Chem. Soc. 134 (2012) 4015–4018. doi:10.1021/ja211630w.

[17] N. Yamasaki, Y. Miyake, H. Yoshida, A. Fujii, M. Ozaki, Solution flow assisted fabrication method of oriented π-conjugated polymer films by using geometrically-asymmetric sandwich structures, Jpn. J. Appl. Phys. 50 020205 (2011). doi:10.1143/JJAP.50.020205.

[18] Y. Yabuuchi, G. Uzurano, M. Nakatani, A. Fujii, M. Ozaki, Uniaxial orientation of poly(3-hexylthiophene) thin films fabricated by the bar-coating method, Jpn. J. Appl. Phys. 58 SBBG04 (2019). doi:10.7567/1347-4065/aafb5d.

[19] B. O'Connor, R.J. Kline, B.R. Conrad, L.J. Richter, D. Gundlach, M.F. Toney, D.M. DeLongchamp, Anisotropic structure and charge transport in highly strain-aligned regioregular poly(3-hexylthiophene), Adv. Funct. Mater. 21 (2011) 3697–3705. doi:10.1002/adfm.201100904.

[20] M. Brinkmann, L. Hartmann, L. Biniek, K. Tremel, N. Kayunkid, Orienting semi-conducting pi-conjugated polymers, Macromol. Rapid Commun. 35 (2014) 9–26. doi:10.1002/marc.201300712.

[21] S. Nagamatsu, W. Takashima, K. Kaneto, Y. Yoshida, N. Tanigaki, K. Yase, K. Omote, Backbone arrangement in "friction-transferred" regioregular poly(3-alkylthiophene)s, Macromolecules. 36 (2003) 5252–5257. doi:10.1021/ma025887t.

[22] T. Morita, V. Singh, S. Nagamatsu, S. Oku, W. Takashima, K. Kaneto, Enhancement of transport characteristics in poly(3-hexylthiophene) films deposited with floating film transfer method, Appl. Phys. Express. 2 (2009) 12–15. doi:10.1143/APEX.2.111502.

[23] A. Dauendorffer, S. Nagamatsu, W. Takashima, K. Kaneto, Optical and transport anisotropy in poly(9,9???-dioctyl-fluorene-alt- bithiophene) films prepared by floating film transfer method, Jpn. J. Appl. Phys. 51 055802 (2012). doi:10.1143/JJAP.51.055802.

[24] M. Pandey, S. Sadakata, S. Nagamatsu, S.S. Pandey, S. Hayase, W. Takashima, Layer-by-layer coating of oriented conjugated polymer films towards anisotropic electronics, Synth. Met. 227 (2017) 29–36. doi:10.1016/j.synthmet.2017.02.018.

[25] A. Tripathi, M. Pandey, S. Nagamatsu, S.S. Pandey, S. Hayase, W. Takashima, Casting Control of Floating-films into Ribbon-shape Structure by modified Dynamic FTM, J. Phys. Conf. Ser. 924 (2017). doi:10.1088/1742-6596/924/1/012014.

[26] A.S.M. Tripathi, M. Pandey, S. Sadakata, S. Nagamatsu, W. Takashima, S. Hayase, S.S. Pandey, Anisotropic charge transport in highly oriented films of semiconducting polymer prepared by ribbon-shaped floating film, Appl. Phys. Lett. 112 123301 (2018). doi:10.1063/1.5000566.

[27] A.S.M. Tripathi, N. Kumari, S. Nagamatsu, S. Hayase, S.S. Pandey, Facile fabrication of large area oriented conjugated polymer films by ribbon-shaped FTM and its implication on anisotropic charge transport, Org. Electron. Physics, Mater. Appl. 65 (2019) 1–7. doi:10.1016/j.orgel.2018.10.043.

[28] A.S.M. Tripathi, S. Sadakata, R.K. Gupta, S. Nagamatsu, Y. Ando, S.S. Pandey, Implication of Molecular Weight on Optical and Charge Transport Anisotropy in PQT-C12 Films Fabricated by Dynamic FTM, ACS Appl. Mater. Interfaces. 11 (2019) 28088–28095. doi:10.1021/acsami.9b06568.

[29] M. Pandey, S. Nagamatsu, W. Takashima, S.S. Pandey, S. Hayase, Interplay of Orientation and Blending: Synergistic Enhancement of Field Effect Mobility in Thiophene-Based Conjugated Polymers, J. Phys. Chem. C. 121 (2017) 11184–11193. doi:10.1021/acs.jpcc.7b03416.

[30] S. Nagamatsu, M. Misaki, M. Chikamatsu, T. Kimura, Y. Yoshida, R. Azumi, N. Tanigaki, K. Yase, Crystal structure of friction-transferred poly(2,5-dioctyloxy-1,4-phenylenevinylene), J. Phys. Chem. B. 111 (2007) 4349–4354. doi:10.1021/jp067555m.

[31] S.C. Lim, S.H. Kim, J.H. Lee, M.K Kim, D.J. Kim, T. Zyung, Surface-treatment effects on organic thin-film transistors , Synthetic Metals 148 (2005) 75-79.doi:10.1166/jnn.2017.12816.

[32] M. Pandey, S.S. Pandey, S. Nagamatsu, S. Hayase, W. Takashima, Controlling Factors for Orientation of Conjugated Polymer Films in Dynamic Floating-Film Transfer Method, J. Nanosci. Nanotechnol. 17 (2017) 1915–1922. doi:10.1166/jnn.2017.12816.

[33] M. Pandey, S. Nagamatsu, S.S. Pandey, S. Hayase, W. Takashima, Orientation Characteristics of Non-regiocontrolled Poly (3-hexyl-thiophene) Film by FTM on Various Liquid Substrates, J. Phys. Conf. Ser. 704 (2016) 012005. doi:10.1088/1742-6596/704/1/012005.

[34] S.S. Pandey, W. Takashima, S. Nagamatsu, T. Endo, M. Rikukawa, K. Kaneto, Regioregularity vs regiorandomness: Effect on photocarrier transport in poly(3-hexylthiophene), Japanese J. Appl. Physics, Part 2 Lett. 39 (2000) 3–7. doi:10.1143/JJAP.39.L94.

[35] K. Tada, K. Miyabe, M. Onada, Sign Inversion of photocarrier in Poly(3-Octadecylthiophene) Associated with Solid-Liquid Phase Transition, Japanese J. Appl. Physics, 41 (2002) pp. L 1422 –L 1424 . doi:10.1143/JJAP.39.L94.

[36] W. Takashima, S.S. Pandey, T. Endo, M. Rikukawa, N. Tanigaki, Y. Yoshida, K. Yase, K. Kaneto, Photocarrier transports related to the morphology of regioregular poly(3-hexylthiophene) films, Thin Solid Films. 393 (2001) 334–342. doi:10.1016/S0040-6090(01)01109-9.

[37] M. Pandey, S.S. Pandey, S. Nagamatsu, S. Hayase, W. Takashima, Influence of backbone structure on orientation of conjugated polymers in the dynamic casting of thin floating-films, Thin Solid Films. 619 (2016) 125–130. doi:10.1016/j.tsf.2016.11.015.

[38] S. Nagamatsu, M. Misaki, T. Kimura, Y. Yoshlda, R. Azumi, N. Tanigaki, K. Yase, Side-chain effects on friction-transferred polymer orientation, Polym. J. 39 (2007) 1300–1305. doi:10.1295/polymj.PJ2007062.

[39] N. Kumari, M. Pandey, K.Hamada, D. Hirotani, S. Nagamatsu, S. Hayase, S.S. Pandey, Role of device architecture and AlOX interlayer in organic Schottky diodes and their interpretation by analytical modeling Role of device architecture and AlO X interlayer in organic Schottky diodes and their interpretation by analytical modeling, J. Appl. Phys,126 (2019)125501. doi:10.1063/1.5109083.

[40] R.C. Nieuwendaal, C.R. Snyder,D.M. Delongchamp, Measuring Order in Regioregular Poly(3-hexylthiophene) with Solid-State ^{13}C CPMAS NMR, *ACS Macro Lett.* 3 (2014) 130-135. doi:10.1063/1.5109083.

[41] D. Sivaramakrishna, M.J. Swamy, Synthesis, characterization and thermotropic phase behavior of a homologous series of N-acyl-l-alaninols and interaction of N-myristoyl l-alaninol with dimyristoylphosphatidylcholine, Chem. Phys. Lipids. 196 (2016) 5–12. doi:10.1016/j.chemphyslip.2016.01.001.

[42] K. Bhargava, A. Bilgaiyan, V. Singh, Two dimensional optoelectronic simulation based comparison of top and bottom contact organic phototransistors, J. Nanosci. Nanotechnol. 15 (2015) 9414-9422. doi:10.1166/jnn.2015.10737.

[43] D. Kiymaz, M. Yagmurcukardes, A. Tomak, H. Sahin, R.T .Senger, F. M. Peeters, H. M. Zareie, C. Zafer. Controlled growth mechanism of poly (3-hexylthiophene) nanowires, Nanotechnoly. 27(2016) 455604. doi:10.1166/jnn.2015.10737.

[44] F.S. Kim, S.A. Jenekhe, Charge Transport in Poly(3-butylthiophene) Nanowires and Their Nanocomposites with an Insulating Polymer, Macromolecules 45 (2012) 7514-7519. doi :10.1021/ma301016c.

[45] K. Kaneto, W.Y. Lim, W. Takashima, T. Endo, M. Rikukawa, Alkyl Chain Length Dependence of Field-Effect Mobilities in Regioregular Poly (3-Alkylthiophene) Films I ’ D (μ A) I D (μA), Jpn. J. Appl. Phys. 39 (2000) L872–L874. doi:10.1063/1.1891301.

[46] M. Pandey, A. Gowda, S. Nagamatsu, S. Kumar, W. Takashima, S. Hayase, S.S. Pandey, Rapid Formation and Macroscopic Self-Assembly of Liquid-Crystalline, High-Mobility, Semiconducting Thienothiophene, Adv. Mater. Interfaces. 5 (2018) 1–11. doi:10.1002/admi.201700875.

[47] J.F. Chang, B. Sun, D.W. Breiby, M.M. Nielsen, T.I. Sölling, M. Giles, I. McCulloch, H. Sirringhaus, Enhanced Mobility of poly(3-hexylthiophene) transistors by spin-coating from high-boiling-point solvents, Chem. Mater. 16 (2004) 4772–4776. doi:10.1021/cm049617w.

[48] M. Pandey, S.S. Pandey, S. Nagamatsu, N. Kumari, Recent Advances in Orientation of Conjugated Polymers for Organic Field-Effect Transistors, J. Mater. Chem. C. 7 (2019) 13323-13351. doi:10.1039/C9TC04397G.

[49] Y. Liu, M. Gibbs, J. Puthussery, S. Gaik, R. Ihly, H.W. Hillhouse, M. Law, Dependence of carrier mobility on nanocrystal size and ligand length in pbse nanocrystal solids, Nano Lett. 10 (2010) 1960–1969. doi:10.1021/nl101284k.

Table 1. Anisotropic electrical parameters deduced from OFETs using thin films of RR-P3AT s with varying alkyl group. Values shown in the parantheses are standard deviations amongst four indepndent devices in each catagories.

RR-P3ATs	Paralll OFETs [$\mu_{\|\|}$] ($cm^2.V^{-1}s^{-1}$)	Perpendicular OFETs [$\mu_{\perp}$] ($cm^2.V^{-1}.s^{-1}$)	($\mu_{\|\|}$ / $\mu_{\perp}$)	I_{ON}/I_{OFF}	DR
P3BT	1.4 (± 0.15) $\times 10^{-2}$	1.0 (± 0.03) $\times 10^{-2}$	1.4	10^3	1.2
P3HT	3.0 (± 0.11) $\times 10^{-2}$	1.7 (± 0.04) $\times 10^{-2}$	1.8	10^4	2.2
P3DT	2.6 (± 0.10)$\times 10^{-2}$	1.9 (± 0.08) $\times 10^{-2}$	1.4	10^4	1.8
P3DDT	2.4 (± 0.07) $\times 10^{-2}$	2.0 (± 0.05) $\times 10^{-2}$	1.2	10^4	1.5
P3ODT	1.9 (± 0.05) $\times 10^{-2}$	1.6 (± 0.05) $\times 10^{-2}$	1.2	10^4	1.1

Figure Captions

Figure 1. Molecular structure of RR-P3ATs (a) and schematic representation of the OFETs fabricated in the BGTC device architecture.

Figure 2. Actual photograph of thin films of RR-P3ATs with varying alkyl chains casted on hydrophilic liquid substrate (Ethylene glycol : Glycerol; 3:1) by ribbon- shaped FTM (a) P3BT, (b) P3HT (c) P3DT (d) P3DDT and (e) P3ODT.

Figure 3. Normalized electronic absorption spectra of spin-coated thin films of RR-P3ATs (a) and polarized electronic absorption spectra of FTM processed thin film of RR-P3HT (b).

Figure 4. Normalized electronic absorption spectra of parallel oriented thin films of RR-P3ATs (a) and influence of alkyl chain length of RR-P3ATs on the extent of molecular orientation (b).

Figure 5. Geometry of the GIXD measurement along with the definition of the scattering vectors (a) and GIXD profile of the RR-P3HT thin films prepared by ribbon-shaped FTM (b).

Figure 6. Out-of-plane X-ray diffraction profile (a) and in-plane GIXD profile (b) of RR-P3AT thin films with varying alkyl chain lengths.

Figure 7. Variation of d-spacing as function of alkyl chain length (a), where red and blue data indicate the experimental and theoretical values of the d-spacing. Schematic representation of the alkyl chain interdigitation, while molecular packing in the RR-P3ATs (b). Dotted lines represent the linear fitting of the theoretical and experimental data.

Figure 8. Typical output characteristics (a) and transfer curve at gate bias of -80 V (b) for the OFETs fabricated using parallel and perpendicularly oriented thin films RR-P3HT prepared by ribbon-shaped FTM.

Figure 9. Schematic representation of implications of face-on and edge-on conformation on the in-plane charge transport applicable to OFETs.

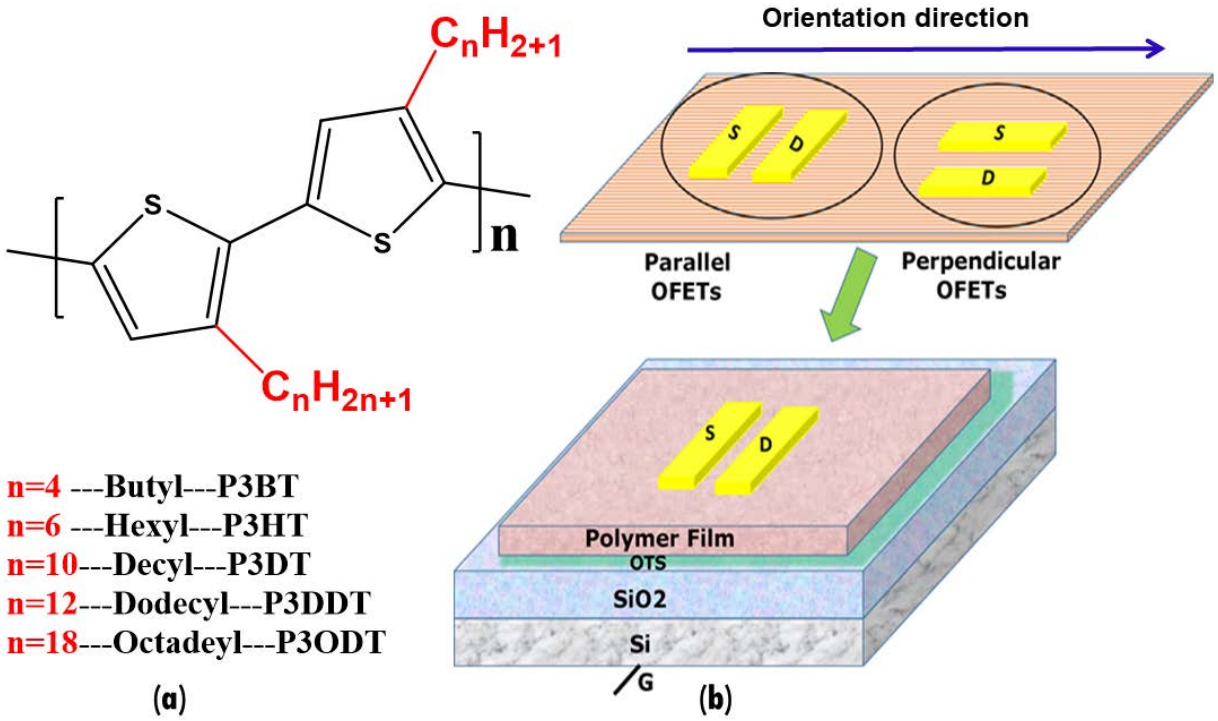

Figure 1

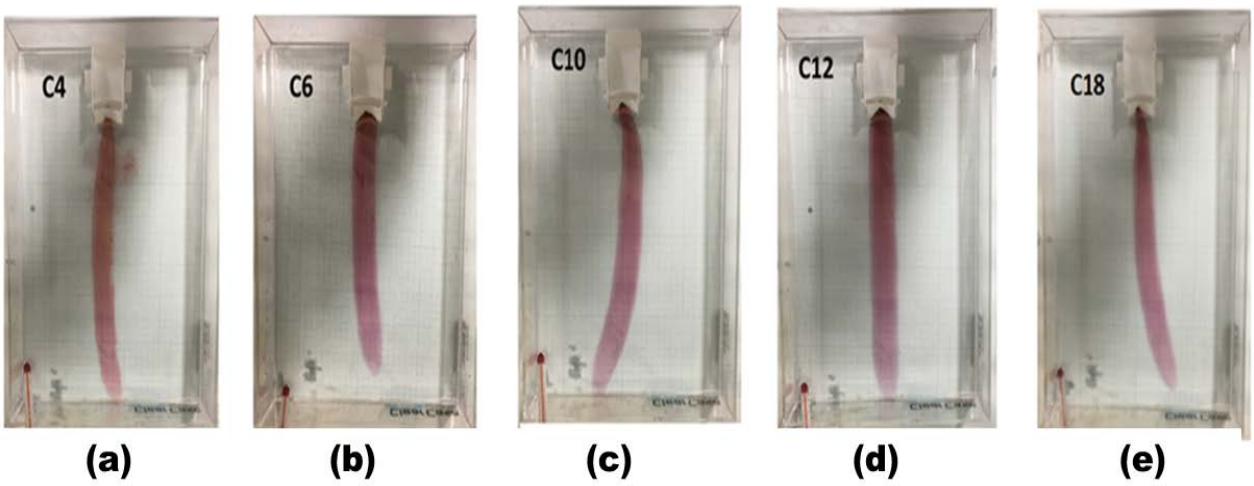

Figure 2

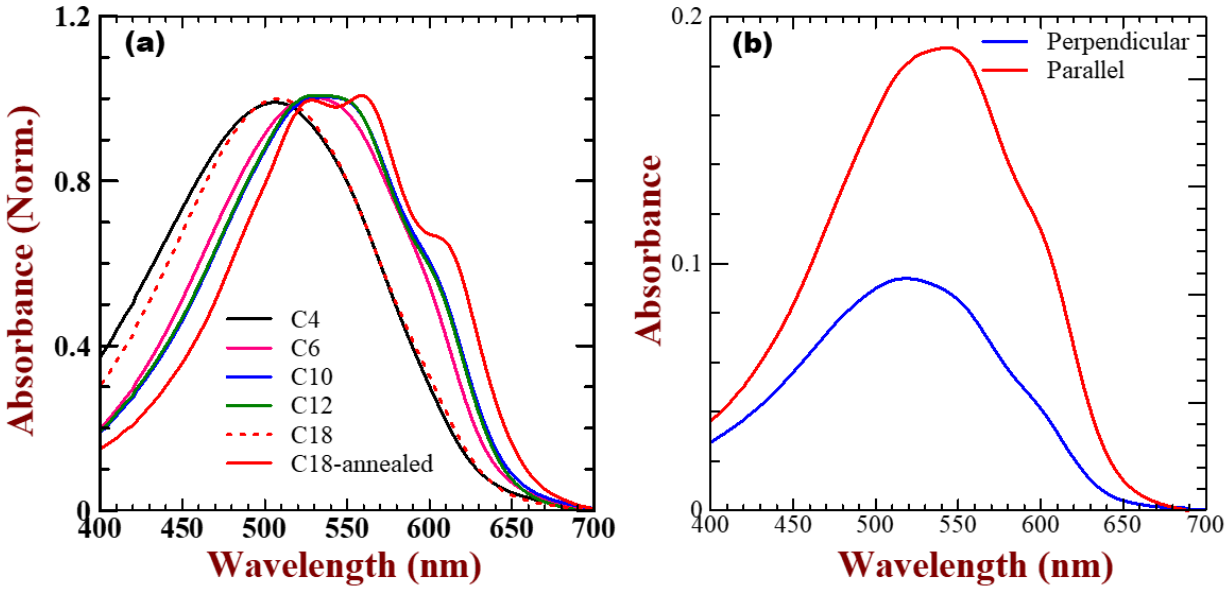

Figure 3

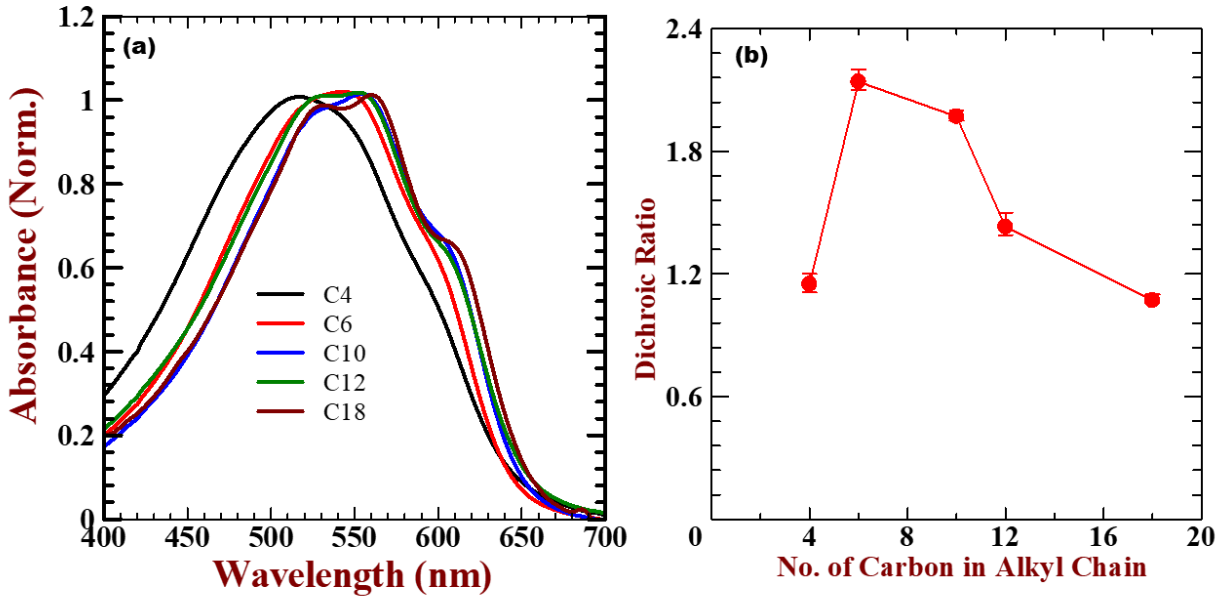

Figure 4

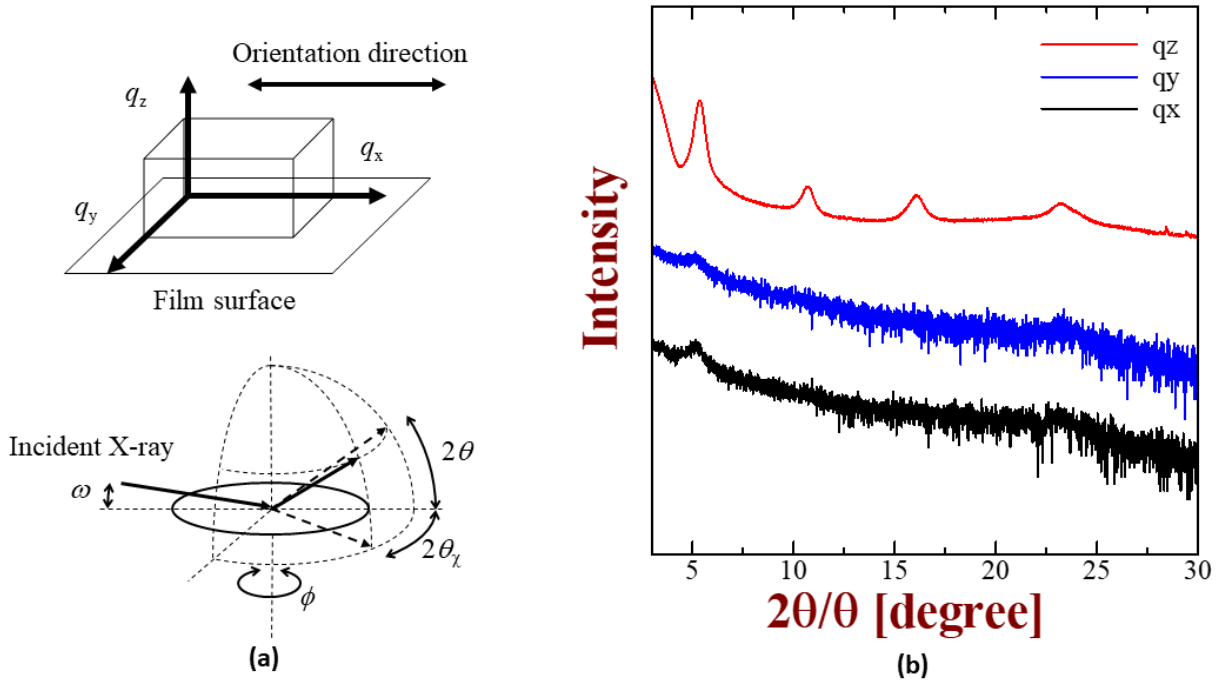

Figure 5

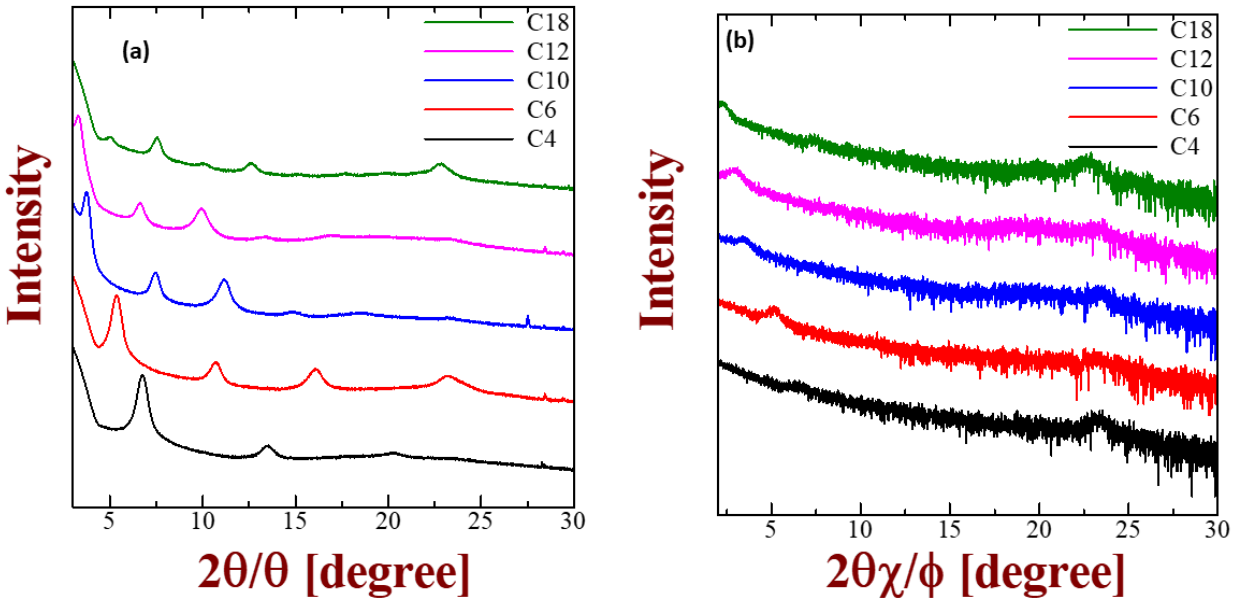

Figure 6

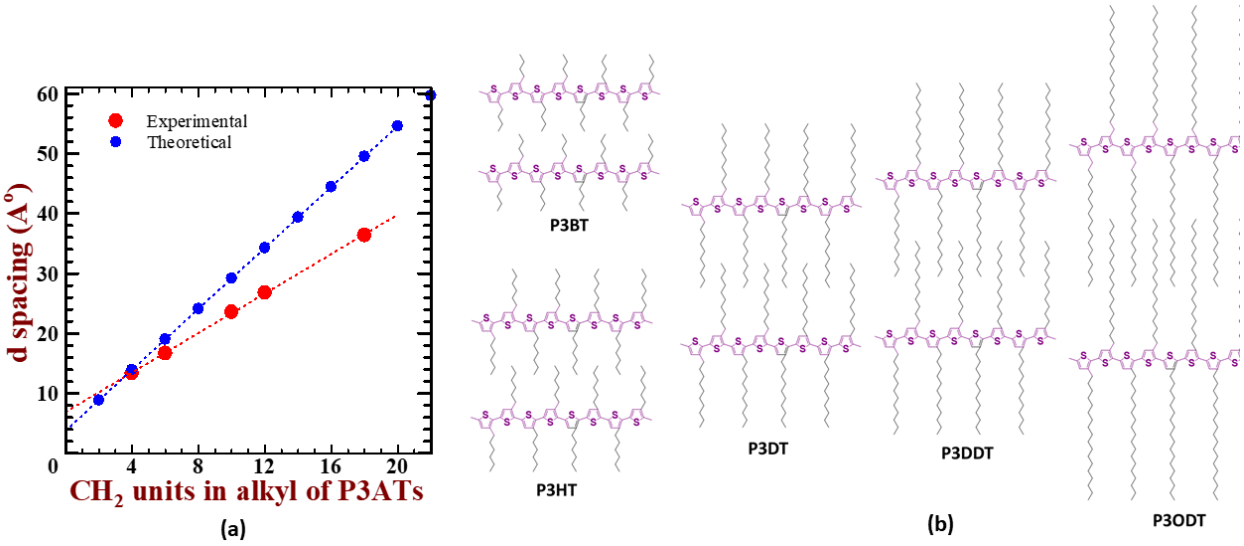

Figure 7

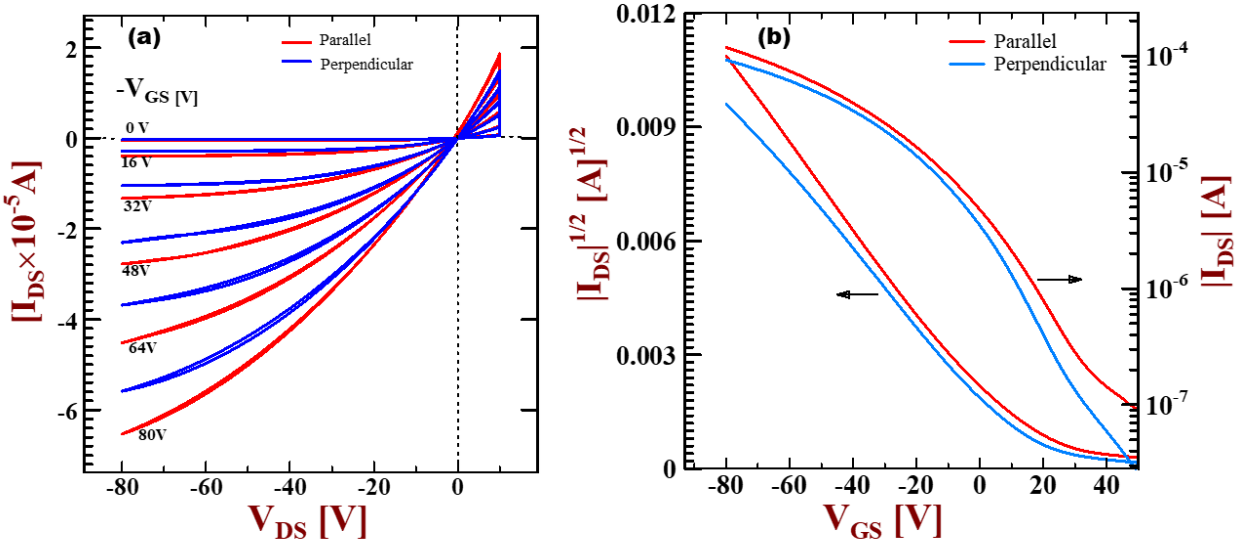

Figure 8

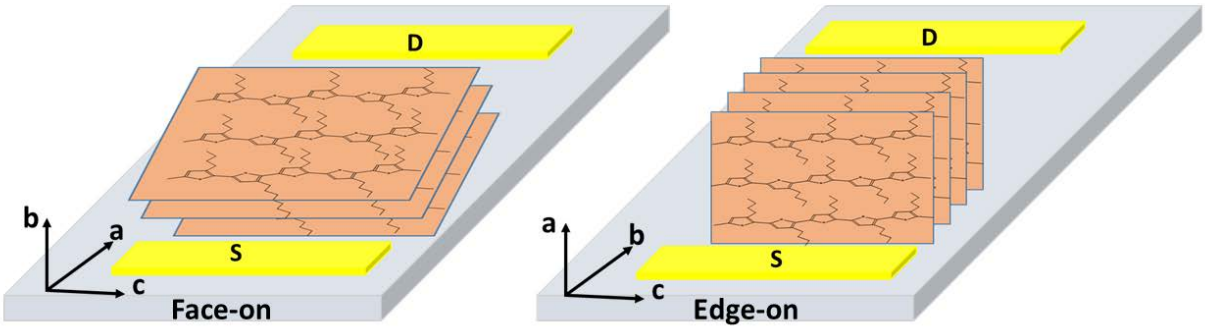

Figure 9

TOC Graphics